

UCSF

UC San Francisco Previously Published Works

Title

Combination Therapy with Radiation and PARP Inhibition Enhances Responsiveness to Anti-PD-1 Therapy in Colorectal Tumor Models.

Permalink

<https://escholarship.org/uc/item/4qd6q18d>

Journal

International Journal of Radiation Oncology - Biology - Physics, 108(1)

Authors

Seyedin, Steven
Hasibuzzaman, M
Pham, Vivan
[et al.](#)

Publication Date

2020-09-01

DOI

10.1016/j.ijrobp.2020.01.030

Peer reviewed



Published in final edited form as:

Int J Radiat Oncol Biol Phys. 2020 September 01; 108(1): 81–92. doi:10.1016/j.ijrobp.2020.01.030.

Combination therapy with radiation and PARP inhibition enhances responsiveness to anti-PD-1 therapy in colorectal tumor models.

Steven N. Seyedin, MD¹, MM Hasibuzzaman, MS², Vivan Pham, BS³, Michael S. Petronek, MS⁴, Cameron Callaghan, MD¹, Amanda L. Kalen, BS⁴, Kranti A Mapuskar, PhD⁴, Sarah L. Mott, MS⁵, Douglas R. Spitz, PhD⁴, Bryan G. Allen, MD/PhD^{1,4}, Joseph M. Caster, MD/PhD^{1,4}

¹Department of Radiation Oncology, University of Iowa Hospital and Clinics, Iowa City, USA

²Interdisciplinary Graduate Program in Human Toxicology, University of Iowa, Iowa City, USA

³Carver College of Medicine, University of Iowa, Iowa City, USA

⁴Free Radical and Radiation Biology Program, Department of Radiation Oncology, University of Iowa Hospital and Clinics, Iowa City, USA

⁵Holden Comprehensive Cancer Center, University of Iowa Hospital and Clinics, Iowa City, Iowa USA

Abstract

Purpose: The majority of colorectal cancers are resistant to cancer immune-checkpoint inhibitors. Ionizing radiation (IR) and several radiosensitizers, including PARP inhibitors, can enhance responsiveness to immune checkpoint inhibitors by potentially complementary mechanisms of action. We assessed the ability of radiation and PARP-inhibition to induce pro-immunogenic changes in tumor cells and enhance their *in vivo* responsiveness to anti-PD-1 antibodies.

Materials and Methods: We performed a candidate drug screen and utilized flow cytometry to assess effects of the PARP inhibitor, veliparib, on IR-mediated changes in MHC-1 antigen presentation and surface localization of immune-modulating proteins including PD-L1 and calreticulin in colorectal cancer tumor models. RT-PCR was used to assess the effects of veliparib and radiation on the expression of proinflammatory and immunosuppressive cytokines. The ability of concurrent PARP inhibition and subablative doses of radiotherapy to enhance *in vivo* responsiveness to anti-PD-1 antibodies was assessed using unilateral flank-tumor models +/- T-cell depletion.

Corresponding Author: Joseph M Caster, Department of Radiation Oncology, University of Iowa Carver College of Medicine, 319-467-5695 (T), 319-356-1530 (F), Joseph-caster@uiowa.edu.

Publisher's Disclaimer: This is a PDF file of an unedited manuscript that has been accepted for publication. As a service to our customers we are providing this early version of the manuscript. The manuscript will undergo copyediting, typesetting, and review of the resulting proof before it is published in its final form. Please note that during the production process errors may be discovered which could affect the content, and all legal disclaimers that apply to the journal pertain.

Conflicts of Interest Statement: None of the authors have any conflicts to disclose

Results: Veliparib was a potent radiosensitizer in both cell lines. Radiation increased surface localization of MHC-1 and PD-L1 in a dose-dependent manner and veliparib pretreatment significantly enhanced these effects with high (8 Gy) but not lower radiation doses. Enhancement of MHC-1 and PD-L1 surface localization by IR and IR + veliparib remained significant 1, 3, and 7 days after treatment. IR significantly increased delayed tumoral expression of pro-inflammatory cytokines INF- γ and CXCL10 but had no significant effect on the expression of IL-6 or TGF- β . Concurrent administration of veliparib and subablative radiotherapy (8 Gy \times 2) significantly prolonged anti-PD-1 mediated *in vivo* tumor growth delay and survival in both tumor models. Moreover, these effects were more pronounced in the microsatellite instability-mutated MC38 tumor model. Enhancement of anti-PD-1 mediated tumor growth delay with veliparib and IR was attenuated by CD8+ T-cell depletion.

Conclusions: We provide preclinical evidence for a novel therapeutic strategy to enhance responsiveness of colorectal tumors to immune checkpoint inhibitors.

Introduction

Cancer immunotherapy with immune checkpoint inhibitors (CPIs), which block inhibitory receptors including CTLA-4 and PD-L1 on the surface of immune cells, have emerged as effective and potentially curative therapies in patients with advanced or metastatic solid tumors¹⁻⁴. Unfortunately, many common solid tumors, including colorectal cancer (CRC), are poorly responsive to CPIs. Despite poor responses, elevated expression of PD-L1 has been noted in 40–60% of CRCs^{5,6}. However, clinical responses to anti-PD-1 therapies are poor except in patients with microsatellite instability (MSI) mutations^{7,8}. This suggests that additional mechanisms of resistance must be overcome to utilize these promising therapies in patients with CRC.

Several approaches to enhancing responsiveness to CPIs in poorly immunogenic tumors have been identified. Ionizing radiation (IR) can enhance systemic tumor control in a phenomenon referred to as the abscopal effect⁹. The mechanism of this enhancement involves a combination of pro-inflammatory effects including enhanced MHC-1-mediated tumor-antigen presentation, increased tumor infiltration by CD8+ T-cells, and reducing immunosuppressive cell populations¹⁰⁻¹⁴. IR also modulates the PD-L1 axis through the CHK1/STAT1/3 pathway in response to the generation of DNA double-strand breaks¹⁵. Several classes of drugs, including inhibitors of PARP and HDACs, can also enhance responsiveness to CPIs. PARP inhibition leads to the accumulation of cytosolic DNA and stimulation of cGAS/STING-mediated type-1 interferon signaling¹⁶. PARP inhibition can also increase PD-L1 levels via ATM/GSK3 β signaling which paradoxically enhances responsiveness to anti-PD-1 therapies in poorly immunogenic murine tumor models¹⁷. The clinical relevance of these findings is supported by two recent clinical investigations of the PARP inhibitor, niraparib, combined with pembrolizumab^{18,19}. Importantly, PARP inhibitors are potent radiosensitizers that enhance the cellular effects of IR. At least one preclinical study has shown that the PARP inhibitor, veliparib, enhances IR-mediated cellular senescence and increases expression of inflammatory cytokines including INF β and CXCL10 in murine B16 melanoma cells²⁰. Collectively, these studies suggest that PARP inhibitors and IR can augment responses to CPIs through distinct and potentially synergistic

mechanisms of action. We hypothesize that this therapeutic combination could be exploited to enhance responsiveness to CPIs in CRC.

Here we show that veliparib and IR can enhance pro-inflammatory cellular effects and responsiveness to anti-PD-1 antibodies in CRC. We utilized two murine CRC tumor models, CT26 and MC38, which represent validated MSS and MSI models of CRC²¹. We investigated the *in vitro* effects of veliparib and IR on tumor surface localization of MHC-1 and the immune-modulating proteins calreticulin and PD-L1 as well as the expression of pro- and anti-inflammatory cytokines. We then assessed the *in vivo* effects of veliparib, IR, and combination therapy on α -PD-1-mediated tumor growth delay and clearance using unilateral flank tumor models. Finally, we used T-cell depletion to confirm that enhanced responsiveness to anti-PD-1 antibodies is dependent upon functional CD8⁺ T-cells. Our data provide preclinical support for a therapeutic strategy that could be readily tested in clinical trials.

Methods and Materials

Cell Culture

Murine CT26 and MC38 cells were generous gifts from the laboratories of Dr. Paloma Giangrande and Dr. Ralph Weichselbaum. CT26 cells were grown in Roswell Park Memorial Institute (RPMI) culture media supplemented with 10% FBS. MC38 cells were grown in Dulbecco's modified culture media supplemented with 10% FBS. Both cell lines were maintained in 4% oxygen at 38°C. Prior to utilization, all cells were confirmed mycoplasma-free by PCR. Both cell lines were used at less than passage 15.

Clonogenic Survival Assays

Clonogenic survival assays and drug treatments were performed as previously described^{22–24}. Cells were plated and allowed to attach for 24 hours. For drug titration, cells were treated for 24 hours with varying concentrations of veliparib (PARP inhibitor), VE-821 (ATR inhibitor), or IPI-549 (PI3K γ isoform inhibitor) or 48 hours with entinostat (HDAC inhibitor) (all obtained from SelleckChem, USA). Cells were trypsinized, counted, plated in fresh media at a concentration of 100–200 cells, and incubated for 7–10 days. Colonies were fixed using 70% ethanol and stained with coomassie blue. Sigmoidal dose-response curves were generated with 4 parameter non-linear regression modeling using Prism Software (Carlsbad, CA) to calculate IC₁₀ and IC₅₀ (doses correlating to 10 and 50% toxicity, respectively). For radiosensitization assays, cells were plated for 24 hours and treated with 5 μ M veliparib, 1 μ M VE821, or 1 μ M IPI-549 for 1 hour and then radiated with 0, 2, 4, or 8 Gy using a Pantak Therapax HF3000 X-ray unit with a maximum X-ray energy of 200 KvP, 15 mA current, beam quality 1 mm Cu, and dose rate of 1.29 Gy/min at an SSD of 50 cm at the University of Iowa core facility. Immediately following radiation, cells were trypsinized and plated in media containing the same concentration of drug and plated in 6 well plates at a density of 100–5000 cells per well. Cells were left in drug-containing media for an additional 23 hours. Cells were incubated for 7–10 days in drug-free media then fixed and stained as above. The linear quadratic formula $SF = e^{-\alpha D - \beta D^2}$ was used to generate survival curves using Prism Software (Carlsbad, CA).

FLOW Cytometry

Cells were plated for 24 hours and treated with radiation (0–8 Gy) +/- 5 μ M veliparib. Cells were trypsinized at indicated time intervals (1, 3, or 7 days) after treatment and washed 3x in 4°C FACS buffer (PBS + 2% BSA). For Calreticulin staining, cells were incubated in primary Calreticulin Polyclonal Antibody (Thermo Fisher Catalog # PA3–900) for 1 hour and washed 3x in PBS. Cells were incubated for 1 hour with either FITC-conjugated anti-MHC-1 mAb (eBioscience, USA), PE-conjugated anti-PDL-1 mAb (eBioscience), and/or secondary DyLight 650-conjugated Donkey anti-Rabbit IgG mAb (Thermo Fisher Catalog # SA5–10041). Stained cells were washed in FACS buffer 3x and resuspended in FACS buffer containing 50 μ g/ml propidium iodide. Unstained cells from all treatment conditions were also analyzed to account for changes in autofluorescence and increased cell diameter following radiation (supplemental figure 1). Data collection was performed on the LSR II flow cytometer (Becton Dickinson, USA) at the core facility of the University of Iowa and data were analyzed with FlowJo software.

RNA Isolation and RT-PCR

Cells were plated for 24 hr and treated as above. At designated times, cells were digested in Trizol reagent (Invitrogen, USA) and RNA was isolated. RNA purity and quantification were assessed using UV spectroscopy at the University of Iowa core facility. cDNA was synthesized using High Fidelity cDNA Synthesis Kits (Applied Biosystems, USA) following the manufacturer's instructions. RT-PCR was performed using POWERUP SYBR green PCR master mix (ThermoFisher Scientific, USA) in a 7900HT light cycler (Applied Biosystems, USA). Relative mRNA expression for each treatment condition was calculated relative to β -actin. Oligonucleotide DNA primers were synthesized (Integrated DNA Technologies, USA) from published primer sequences (supplemental table 1)^{20,25,26}.

In Vivo Studies

Eight-week-old male and female C57bl/6 and BALB/c mice were purchased from Jackson Laboratories (USA) and housed/handled in accordance with the University of Iowa Institutional Animal Care and Use Committee (IACUC). 1.0×10^6 MC38 and CT26 cells were resuspended in a 50/50 volume of PBS and matrigel and subcutaneously injected into the left flanks of C57bl/6 and BALB/c mice. Mice were randomly assigned to experimental groups (5–12 mice per group) when tumors reached approximately 5 mm in diameter. Veliparib (25 mg/kg) was administered P.O. via oral gavage BID for a total of six consecutive days starting two days before radiation. Anti-PD-1 antibodies (clone RMP1–14, BioXcell, USA) were administered at a dose of 200 μ g I.P. every 72 hours for a total of 3 doses starting the first day of radiation. Radiation (8 Gy \times 2 fractions separated by 48 hours) was delivered a Pantak Therapax HF3000 X-ray unit with a maximum X-ray energy of 200 KvP, 15 mA current, beam quality 1 mm Cu, and dose rate of 1.29 Gy/min at an SSD of 50 cm at the University of Iowa Core. For radiation, mice were anesthetized using ketamine/xylozine (100/10 mg/kg) and shielded with 3 mm lead. T-cell depletion was accomplished by I.P. administration of anti-CD8 antibodies (clone 2.43, BioXcell) at a dose of 250 μ g starting when tumors reach 5 mm in diameter and continued every 72 hours until study completion. Animals were sacrificed whenever tumors reached 2.0 cm in largest diameter,

significant skin ulceration was noted, or they displayed any signs of distress or limited mobility. Tumor volumes were assessed every 2–3 days after completion of treatment by measuring the tumor length and width and using the formula $Tv = L \times 1/2W^2$. For survival studies, animals were censored when they met study endpoints or died.

Statistics

Effects of veliparib pretreatment and radiation on median fluorescence intensity (MFI) of cell-surface markers (MHC-1, calreticulin, and PD-L1) were assessed using 2-way ANOVAs with variables of drug and radiation dose using Prism Software. Effects of veliparib and radiation on mRNA expression were assessed using 2-way ANOVAs with variables of treatment and time. Effects were considered significant at $p < 0.05$. All changes in MRI expression $< \pm$ two-fold compared to control were considered insignificant. Post-hoc analyses using Tukey's T-test were performed when significant main effects were identified. Linear mixed effects regression models were used to estimate and compare *in vivo* CT26 tumor growth curves. Owing to the longer initial tumor growth delay, non-linear mixed effects regression models were used to estimate and compare *in vivo* MC38 tumor growth curves. Pairwise comparisons were performed to identify specific group differences in the growth curves. All tests were two-sided and carried out at the 5% level of significance using SAS v9.4 (SAS Institute, Cary, NC). Survival estimates were generated using the Kaplan-Meier method and compared by log-rank analysis (Prism Software).

Results

Candidate Drug Screen

We selected 4 candidate radiosensitizers and assessed *in vitro* toxicity in MC38 and CT26 tumor cells: the PARP inhibitor veliparib, the HDAC inhibitor entinostat, the PI3K- γ isoform inhibitor IPI549, and the ATR inhibitor VE-821. We performed monotherapy dose-titration studies to identify minimally toxic doses (IC10) of each drug in both models (Fig 1a–b; Table 1). We then tested the radiosensitizing potential of each drug in both cell lines (Fig 1c–d; Table 1). IPI-549 did not enhance radiosensitivity in either cell line. Entinostat significantly enhanced radiosensitivity in CT26 but not MC38 cells. VE821 and veliparib were potent radiosensitizers in both cell lines. We selected veliparib as our model drug for two reasons. First, veliparib has direct clinical relevance as a radiosensitizer for rectal tumors as it has been tested in combination with preoperative chemoradiation for the management of locally-advanced rectal cancers in the NRG GI002 clinical study. Second, PARP inhibitors have direct clinical relevance to CPIs as they have been utilized in clinical trials aiming to enhance responsiveness to anti-PD-1 therapies in poorly responsive tumors^{18,19}.

IR and Veliparib Increase Tumor Antigen Presentation

We assessed the effects of IR and veliparib on antigen presentation by assessing MHC-1 (H-2D subunit) surface localization (Fig 2a–d). IR dose-dependently increased MHC-1 surface localization in both cell lines ($p < 0.01$ for main effect of dose). MHC-1 surface localization was significantly increased compared to control following doses of 4 and 8 Gy in both cell lines ($p < 0.05$ for both). Veliparib pretreatment significantly increased radiation-

mediated MHC-1 surface localization following high (8 Gy) but not lower doses of radiation ($p < 0.01$). We then assessed if changes in MHC-1 surface localization were mediated by changes in expression of MHC-1 (H-2D subunit) or associated antigen processing proteins TAP-1 or $\beta 2$ -macroglobulin (Fig 2e–f). Neither IR, veliparib, nor combination therapy induced significant changes in expression of any of these genes. However, it is worth noting that changes in MHC-1 H-2D subunit expression were quantitatively similar to changes in MHC-1 surface localization 24 hours after radiation and veliparib treatment which suggests changes in MHC-1 subunit transcription could at least partially mediate enhanced surface localization after radiation and PARP inhibition. We next assessed the effects of veliparib and IR on MHC-1 surface localization at later times (3 and 7 days) after treatment (Fig 2g–h). MHC-1 surface localization remained significantly increased following treatment with IR or IR + Veliparib compared to control or veliparib at both 3 and 7 days in both cell lines ($P < 0.01$ for both). In CT26 tumors, veliparib pretreatment significantly increased MHC-1 surface localization more than IR alone after 1 day and we observed a non-significant trend towards increased MHC-1 surface localization with veliparib pretreatment at 3 and 7 days post IR. In MC38 tumors, MHC-1 surface localization was significantly higher after veliparib pretreatment compared to IR 1 and 3 days after pretreatment. At 7 days, there was no significant difference between IR and IR + veliparib. We also observed a significant main effect of time ($P < 0.01$) and post-hoc analysis showed significantly more MHC-1 surface localization at 7 than 1 days for both IR and IR + veliparib.

Veliparib Enhances IR-Induced Inflammatory Cytokine Signaling

We next assessed the *in vitro* effects of IR and veliparib on tumoral expression of inflammatory cytokines and chemokines. Cells were treated with veliparib, IR (8 Gy), or veliparib + IR and expression of INF- β , CXCL-10, IL-6, and TGF- β were assessed 1, 3, and 7 days after treatment (Figure 3). IR stimulated robust and delayed increases in the expression of INF- β and CXCL10 in both cell lines. In CT26 cells (Fig. 3a), expression of INF- β and CXCL10 was significantly increased compared to veliparib alone and control 7 days after radiation treatment ($p < 0.01$) and veliparib pretreatment significantly increased expression of both genes more than radiation alone ($p < 0.01$ for both). IR with or without veliparib did not significantly affect expression of IL-6 or TGF- β at any timepoint. We observed similar results in MC38 cells although the timing of enhanced gene expression was different (Fig. 3b). Expression of INF- β and CXCL10 were markedly increased 3 but not 1 or 7 days after IR. INF- β expression was significantly enhanced with veliparib pretreatment compared to IR alone ($p < 0.03$).

PARP Inhibition Modulates IR-induced Changes in Immunomodulatory Proteins

We then assessed the effects of IR and veliparib on surface localization of the immunomodulating proteins, PD-L1 and calreticulin (Fig. 4). IR dose-dependently increased PD-L1 surface localization in both cell lines after 24 hours ($p < 0.01$) (Fig. 4a–b) and this effect was significantly enhanced by veliparib pretreatment and high-dose (8 Gy) IR ($p < 0.01$). We then assessed PD-L1 surface localization at later time points (3 and 7 days) after treatment with veliparib, IR, and IR + veliparib (Fig 4c–d). In CT26 cells, PD-L1 surface localization remained significantly increased after IR and IR + Veliparib compared to control at all timepoints ($P < 0.05$ for both) but the difference between IR alone and IR + veliparib was

only significant at the 24 hour timepoint. In MC38 cells, veliparib + IR increased PD-L1 surface localization more than IR alone 1 and 3 days after treatment ($P < 0.01$ for 1 day and $P < 0.05$ for 3 days). PD-L1 surface localization significantly increased over the course of 7 days after treatment with IR and IR + veliparib ($P < 0.05$ for main effect of time) but there was no significant difference between the two treatments at 7 days. High-dose (8 Gy) IR significantly increased calreticulin surface localization in CT26 cells ($p < 0.01$) but not MC38 cells after 24 hours. Veliparib pretreatment did not significantly increase radiation-mediated calreticulin surface localization in either cell line (Fig. 4e–f).

Sub-ablative IR and PARP Inhibition Enhance *In Vivo* Efficacy of α -PD-1 Antibodies

We assessed the ability of veliparib and sub-ablative high-dose IR to enhance responsiveness to anti-PD-1 therapy using unilateral CT26 and MC38 flank tumors (Fig. 5). The treatment scheme is shown in Figure 5a. Neither veliparib, RMP-1–14, or veliparib + RMP1–14 had any significant effect on tumor growth or survival without radiation in CT26 tumors (Fig. 5b,d; supplemental fig. 2). IR significantly prolonged CT26 tumor growth delay and survival compared to control ($p < 0.001$) and combination therapy with IR + veliparib + RMP1–14 significantly prolonged tumor growth delay and enhanced survival more than all other treatments ($P < 0.04$). These effects were largely transient as only 1/11 CT26-bearing mice treated with triple therapy achieved complete tumor regression. In contrast, MSI-mutated MC38 tumors were more responsive to anti-PD-1 therapy (Fig. 5c,e; supplemental Fig. 3). Treatment with RMP1–14 alone significantly prolonged tumor growth delay and survival compared to saline control or veliparib alone ($p < 0.01$) but did not stimulate any complete responses. Treatment with IR + RMP1–14 trended to prolong tumor growth delay longer than IR alone ($p = 0.26$), significantly prolonged survival ($P < 0.03$) and resulted in 2/7 (28.5%) complete tumor responses. Combination therapy with veliparib + IR + RPM-1–14 produced significantly longer tumor growth delay than all other treatments ($p < 0.01$) and 8/10 (80%) mice achieved complete tumor regression. We also assessed the effects of concurrent radiation and anti-PD-1 therapy by delaying RMP1–14 administration until 1 week after receipt of radiation. Delaying RMP1–14 resulted in significantly inferior tumor growth delay ($P < 0.01$), survival ($P < 0.01$), and complete responses (4/9) compared to concurrent administration. We tested the hypothesis that enhancement of anti-PD-1 efficacy by combination veliparib and IR was immune-mediated using T-cell depletion (Fig 5F; supplemental Fig. 4). MC38-bearing mice were treated with IR, veliparib, and RMP1–14 as above +/- T-cell depletion. T-cell depletion did not significantly affect local control compared to saline controls. However, T-cell depletion did significantly attenuate tumor growth delay in animals treated with IR + veliparib + RMP1–14 ($p < 0.01$).

Discussion

In the present study, we demonstrate that concurrent IR and PARP inhibition can enhance responsiveness to CPIs in murine models of rectal cancer. Our data provide preclinical evidence for a novel therapeutic strategy that can be assessed in prospective clinical trials. A major strength of our study is that we utilized two syngeneic models of rectal cancer, CT26 and MC38, which have been validated as MSS and MSI tumor models, respectively. The presence of microsatellite instability mutations has been identified as the most important

known predictor of responses to CPIs in metastatic colorectal cancers^{7,8}. Overall response rates to anti-PD-1 monotherapy are approximately 30% in MSI mutated tumors and <5% in non-mutated tumors. This difference in responsiveness is believed to be mediated by a higher mutational burden in MSI CRCs. Efremova et al. recently performed whole exome sequencing of MC38 tumors and identified 1399 unique tumor neoantigens that were predicted to bind strongly to MHC-1²¹. In contrast, Castle et al. found that CT26 tumors harbor approximately one order of magnitude fewer tumor neoantigens²⁷. Despite these significant differences in neoantigen burden, we showed here that PARP inhibition and IR increase CPI-mediated local tumor control in both MSS and MSI tumor models. The magnitude of this effect was more pronounced in MSI MC38 tumors even though we observed roughly equivalent increases in MHC-1 antigen presentation with combination therapy in both tumor models. This observation supports the hypothesis that interventions which increase tumor antigen presentation will be most effective in tumors with proportionally higher antigenic diversity. Nonetheless, our data suggest that this approach may still be effective for tumors with relatively low mutational burdens including MSS CRCs. The principle difference in therapeutic responses between the model systems is that tumor growth delay was largely transient in MSS CT26 tumors. One possible interpretation is that while combination therapy can stimulate anti-tumor responses in CT26 tumors, these are more susceptible to additional mechanisms of resistance. Potential strategies to address these could include approaches to further maximize neoantigen presentation or minimize the effects of immunosuppressive subpopulations in the tumor microenvironment.

We also showed that enhancement of tumor antigen presentation and PD-L1 protein by IR and PARP inhibition is strongly dose-dependent. Conventional radiotherapy doses of approximately 2 Gy had no significant effect on MHC-1 or PD-L1 surface localization whereas both were significantly increased following higher doses of radiation (4–8 Gy). While the optimal dose-fractionation for stimulating systemic immune-responses with IR has not been clearly established, multiple preclinical studies have suggested that fraction sizes in the range of 5–12 Gy are probably more effective than higher or lower doses^{28–32} and our data support this. Fractions less than 5 Gy are stimulate inferior tumor infiltration by CD8+ T-cells^{29,33} whereas doses higher than 12–18 Gy stimulate expression of the DNA exonuclease TREX-1 that attenuates IR-mediated induction of type 1 INF signaling³². Many ongoing clinical trials combining IR and CPIs utilize SBRT dosing to stimulate abscopal responses in patients with metastatic disease. However, there is growing interest in utilizing IR and CPIs in the definitive setting and rectal cancer may be the ideal clinical entity to test this approach. For rectal cancer, short course hypofractionated radiotherapy (5 Gy/day × 5 fractions) is a well-established alternative pre-operative paradigm that provides equivalent pathologic responsiveness to conventional long-course radiotherapy³⁴. Hypofractionated regimens like this may provide more effective enhancement of pathologic responses to CPIs than conventional long-course radiation by increasing radiation-mediated neoantigen presentation and tumoral T-cell infiltration.

In addition to uncertainties related to radiation dose, the optimal sequencing of CPIs and IR is also unclear, especially in the setting of additional agents. Adjuvant CPI therapy initiated after completion of definitive chemoradiotherapy improves long-term disease control and survival in immunogenic histologies including NSCLC³. We showed here that delayed

administration of CPIs until 1 week after completion of IR does significantly improve local control and survival compared to IR and veliparib alone. However, delayed administration of anti-PD-1 antibodies was significantly inferior to concurrent administration in terms of both local control and survival. We observed complete and durable tumor regression in 80 and 40% of mice treated with concurrent and delayed RMP1–14, respectively. This observation suggests that clinical approaches aimed at utilizing CPIs and radiosensitizers to maximize pathologic responses might be more effective with concurrent than adjuvant CPI administration.

Our results demonstrate that IR and PARP inhibition can improve local tumor control when combined with CPIs. However, it is currently unclear if this approach also improves systemic disease control. Using T-cell depletion studies, we demonstrated that enhanced tumor control to combination therapy is immune-mediated and dependent upon CD8+ T-cells. We predict that these represent adaptive antitumor immune responses that could also stimulate abscopal responses outside of the radiation field. At present, this hypothesis is speculative and the therapeutic benefit of combination therapy with IR, PARP inhibition, and CPIs in patients with metastatic disease is unclear. However rectal cancer is one clinical entity in which improved local control and pathologic responsiveness is a clinically meaningful endpoint. Surgical resection is associated with numerous long-term toxicities. Prospective trials have shown that surgical resection may not be necessary for patients who achieve clinical complete responses to neoadjuvant chemoradiotherapy^{35–37}. Therefore, therapeutic approaches which significantly enhance local tumor control could directly impact patient care and improve quality of life by increasing the proportion of patients eligible for organ preservation irrespective of their effects on distant disease control.

There is a growing clinical interest in utilizing novel radiosensitizers which inhibit specific DNA repair pathway proteins including PARP, ATM, ATR, and DNA-PK. In the present study, we utilized veliparib as a model drug because PARP inhibitors, including veliparib, have direct clinical relevance with rectal cancer and CPIs. However, it is currently unclear how our observations with veliparib apply to specific inhibitors of other DNA repair pathways. While these proteins share many common signaling pathways, there are potentially important differences between them that may affect immune responses to IR. PARP inhibition increases PD-L1 surface localization by decreasing GSK3 β -mediated ubiquitination of PD-L1¹⁷. However, this is dependent upon detection of double strand DNA damage by ATM. Inhibition of ATR has also been shown to attenuate IR-mediated enhancement of PD-L1 surface localization³⁸. This suggests that inhibitors of ATM or ATR may be less dependent upon concurrent CPIs than PARP inhibitors to enhance the local effects of IR. Future investigations in our laboratory will seek to understand how inhibitors of specific DNA repair pathways interact with emerging immunotherapies to identify the most promising combinations for testing in clinical trials.

Our study has several important limitations. We utilized MHC-1 surface localization as a measure of radiation-mediated tumor antigen presentation. However, only a very small percentage MHC-1 associated peptides are unique tumor neoantigens¹¹. Our results suggest that veliparib may enhance tumor antigen processing and presentation in response to IR. However, this hypothesis is speculative because we did not sequence MHC-1 associated

peptides to prove that veliparib pretreatment enhances the diversity or quantity of unique peptide sequences compared to radiation alone. Similarly, while we provide evidence that veliparib and IR induce changes in tumors that could enhance susceptibility to CPIs, these observations are correlative. Tumor cells are only one component of the TME that can modulate immune cell functions. It is unclear how PARP inhibitors and IR affect the composition of various immune components within the TME which could impact responsiveness to CPIs as much or more than tumor cells. Understanding how IR and radiosensitizers mechanistically modulate responsiveness to CPIs could improve our understanding of resistance to immunotherapy and enable novel hypothesis-driven approaches to overcome them. Finally, our study utilized murine tumor models as studies investigating *in vivo* responses to CPIs require immunocompetent model systems. The relevance of our observations to human tumors could be improved by showing that PARP inhibition and IR stimulate similar *in vitro* changes in the immunophenotype in murine and human colorectal tumor cells.

In conclusion, we provide preclinical evidence of a novel therapeutic approach to enhance local responsiveness to CPIs in both MSS and MSI colorectal cancers. Enhanced local tumor control with IR, PARP inhibition, and anti-PD-1 therapy could provide clinically-meaningful benefits for patients with locally-advanced rectal cancer. Multiple PARP inhibitors are clinically available and this hypothesis could be readily tested in prospective clinical trials.

Supplementary Material

Refer to Web version on PubMed Central for supplementary material.

Acknowledgements:

Data presented herein were obtained at the Genomics Division of the Iowa Institute of Human Genetics which is supported, in part, by the University of Iowa Carver College of Medicine and the Holden Comprehensive Cancer Center (National Cancer Institute of the National Institutes of Health under Award Number P30CA086862).

The data presented herein were obtained at the Flow Cytometry Facility, which is a Carver College of Medicine / Holden Comprehensive Cancer Center core research facility at the University of Iowa. The facility is funded through user fees and the generous financial support of the Carver College of Medicine, Holden Comprehensive Cancer Center, and Iowa City Veteran's Administration Medical Center. Research reported in this publication was supported by the National Cancer Institute of the National Institutes of Health under Award Number P30CA086862

Funding: This work was supported by NIH Grant RO1CA182804 and Grant IRG-15-176-41 from the American Cancer Society administered through the Holden Comprehensive Cancer Center at the University of Iowa.

References:

1. Wolchok JD, Chiarion-Sileni V, Gonzalez R, et al. Overall Survival with Combined Nivolumab and Ipilimumab in Advanced Melanoma. *The New England journal of medicine*. 10 5 2017;377(14):1345–1356. [PubMed: 28889792]
2. Hodi FS, O'Day SJ, McDermott DF, et al. Improved survival with ipilimumab in patients with metastatic melanoma. *The New England journal of medicine*. 8 19 2010;363(8):711–723. [PubMed: 20525992]
3. Antonia SJ, Villegas A, Daniel D, et al. Overall Survival with Durvalumab after Chemoradiotherapy in Stage III NSCLC. *The New England journal of medicine*. 12 13 2018;379(24):2342–2350. [PubMed: 30280658]

4. Paz-Ares L, Luft A, Vicente D, et al. Pembrolizumab plus Chemotherapy for Squamous Non-Small-Cell Lung Cancer. *The New England journal of medicine*. 11 22 2018;379(21):2040–2051. [PubMed: 30280635]
5. Li Y, Liang L, Dai W, et al. Prognostic impact of programmed cell death-1 (PD-1) and PD-ligand 1 (PD-L1) expression in cancer cells and tumor infiltrating lymphocytes in colorectal cancer. *Molecular cancer*. 8 24 2016;15(1):55. [PubMed: 27552968]
6. Valentini AM, Di Pinto F, Cariola F, et al. PD-L1 expression in colorectal cancer defines three subsets of tumor immune microenvironments. *Oncotarget*. 2 2 2018;9(9):8584–8596. [PubMed: 29492219]
7. Le DT, Uram JN, Wang H, et al. PD-1 Blockade in Tumors with Mismatch-Repair Deficiency. *The New England journal of medicine*. 6 25 2015;372(26):2509–2520. [PubMed: 26028255]
8. Overman MJ, McDermott R, Leach JL, et al. Nivolumab in patients with metastatic DNA mismatch repair-deficient or microsatellite instability-high colorectal cancer (CheckMate 142): an open-label, multicentre, phase 2 study. *The Lancet. Oncology* 9 2017;18(9):1182–1191. [PubMed: 28734759]
9. Formenti SC, Rudqvist NP, Golden E, et al. Radiotherapy induces responses of lung cancer to CTLA-4 blockade. *Nature medicine*. 12 2018;24(12):1845–1851.
10. Aguilera TA, Rafat M, Castellini L, et al. Reprogramming the immunological microenvironment through radiation and targeting Axl. *Nature communications*. 12 23 2016;7:13898.
11. Reits EA, Hodge JW, Herberts CA, et al. Radiation modulates the peptide repertoire, enhances MHC class I expression, and induces successful antitumor immunotherapy. *The Journal of experimental medicine*. 5 15 2006;203(5):1259–1271. [PubMed: 16636135]
12. Filatenkov A, Baker J, Mueller AM, et al. Ablative Tumor Radiation Can Change the Tumor Immune Cell Microenvironment to Induce Durable Complete Remissions. *Clinical cancer research : an official journal of the American Association for Cancer Research*. 8 15 2015;21(16):3727–3739. [PubMed: 25869387]
13. Twyman-Saint Victor C, Rech AJ, Maity A, et al. Radiation and dual checkpoint blockade activate non-redundant immune mechanisms in cancer. *Nature*. 4 16 2015;520(7547):373–377. [PubMed: 25754329]
14. Sharabi AB, Nirschl CJ, Kochel CM, et al. Stereotactic Radiation Therapy Augments Antigen-Specific PD-1-Mediated Antitumor Immune Responses via Cross-Presentation of Tumor Antigen. *Cancer immunology research*. Apr 2015;3(4):345–355.
15. Sato H, Niimi A, Yasuhara T, et al. DNA double-strand break repair pathway regulates PD-L1 expression in cancer cells. *Nature communications*. 11 24 2017;8(1):1751.
16. Huang J, Wang L, Cong Z, et al. The PARP1 inhibitor BMN 673 exhibits immunoregulatory effects in a Brca1(−/−) murine model of ovarian cancer. *Biochemical and biophysical research communications*. 8 7 2015;463(4):551–556. [PubMed: 26047697]
17. Jiao S, Xia W, Yamaguchi H, et al. PARP Inhibitor Upregulates PD-L1 Expression and Enhances Cancer-Associated Immunosuppression. *Clinical cancer research : an official journal of the American Association for Cancer Research*. 7 15 2017;23(14):3711–3720. [PubMed: 28167507]
18. Vinayak S, Tolaney SM, Schwartzberg L, et al. Open-Label Clinical Trial of Niraparib Combined With Pembrolizumab for Treatment of Advanced or Metastatic Triple-Negative Breast Cancer. *JAMA oncology*. 6 13 2019.
19. Konstantinopoulos PA, Waggoner S, Vidal GA, et al. Single-Arm Phases 1 and 2 Trial of Niraparib in Combination With Pembrolizumab in Patients With Recurrent Platinum-Resistant Ovarian Carcinoma. *JAMA oncology*. 6 13 2019.
20. Meng Y, Efimova EV, Hamzeh KW, et al. Radiation-inducible immunotherapy for cancer: senescent tumor cells as a cancer vaccine. *Molecular therapy : the journal of the American Society of Gene Therapy*. 5 2012;20(5):1046–1055. [PubMed: 22334019]
21. Efremova M, Rieder D, Klepsch V, et al. Targeting immune checkpoints potentiates immunoeediting and changes the dynamics of tumor evolution. *Nature communications*. 1 2 2018;9(1):32.
22. O'Leary BR, Houwen FK, Johnson CL, et al. Pharmacological Ascorbate as an Adjuvant for Enhancing Radiation-Chemotherapy Responses in Gastric Adenocarcinoma. *Radiation research*. 5 2018;189(5):456–465. [PubMed: 29547353]

23. Camphausen K, Burgan W, Cerra M, et al. Enhanced radiation-induced cell killing and prolongation of gammaH2AX foci expression by the histone deacetylase inhibitor MS-275. *Cancer research*. 1 1 2004;64(1):316–321. [PubMed: 14729640]
24. Caster JM, Yu SK, Patel AN, et al. Effect of particle size on the biodistribution, toxicity, and efficacy of drug-loaded polymeric nanoparticles in chemoradiotherapy. *Nanomedicine : nanotechnology, biology, and medicine*. 7 2017;13(5):1673–1683.
25. Kim K, Skora AD, Li Z, et al. Eradication of metastatic mouse cancers resistant to immune checkpoint blockade by suppression of myeloid-derived cells. *Proceedings of the National Academy of Sciences of the United States of America*. 8 12 2014;111(32):11774–11779. [PubMed: 25071169]
26. Wickert L, Steinkruger S, Abiaka M, et al. Quantitative monitoring of the mRNA expression pattern of the TGF-beta-isoforms (beta 1, beta 2, beta 3) during transdifferentiation of hepatic stellate cells using a newly developed real-time SYBR Green PCR. *Biochemical and biophysical research communications*. 7 12 2002;295(2):330–335. [PubMed: 12150952]
27. Castle JC, Loewer M, Boegel S, et al. Immunomic, genomic and transcriptomic characterization of CT26 colorectal carcinoma. *BMC genomics*. 3 13 2014;15:190. [PubMed: 24621249]
28. Chakraborty M, Abrams SI, Coleman CN, Camphausen K, Schlom J, Hodge JW. External beam radiation of tumors alters phenotype of tumor cells to render them susceptible to vaccine-mediated T-cell killing. *Cancer research*. 6 15 2004;64(12):4328–4337. [PubMed: 15205348]
29. Schaeue D, Ratikan JA, Iwamoto KS, McBride WH. Maximizing tumor immunity with fractionated radiation. *International journal of radiation oncology, biology, physics*. 7 15 2012;83(4):1306–1310.
30. Dewan MZ, Galloway AE, Kawashima N, et al. Fractionated but not single-dose radiotherapy induces an immune-mediated abscopal effect when combined with anti-CTLA-4 antibody. *Clinical cancer research : an official journal of the American Association for Cancer Research*. 9 1 2009;15(17):5379–5388. [PubMed: 19706802]
31. Verbrugge I, Hagekyriakou J, Sharp LL, et al. Radiotherapy increases the permissiveness of established mammary tumors to rejection by immunomodulatory antibodies. *Cancer research*. 7 1 2012;72(13):3163–3174. [PubMed: 22570253]
32. Vanpouille-Box C, Alard A, Aryankalayil MJ, et al. DNA exonuclease Trex1 regulates radiotherapy-induced tumour immunogenicity. *Nature communications*. 6 9 2017;8:15618.
33. Lugade AA, Moran JP, Gerber SA, Rose RC, Frelinger JG, Lord EM. Local radiation therapy of B16 melanoma tumors increases the generation of tumor antigen-specific effector cells that traffic to the tumor. *Journal of immunology*. 6 15 2005;174(12):7516–7523.
34. Erlandsson J, Holm T, Pettersson D, et al. Optimal fractionation of preoperative radiotherapy and timing to surgery for rectal cancer (Stockholm III): a multicentre, randomised, non-blinded, phase 3, non-inferiority trial. *The Lancet. Oncology* 3 2017;18(3):336–346. [PubMed: 28190762]
35. Habr-Gama A, Perez RO, Nadalin W, et al. Operative versus nonoperative treatment for stage 0 distal rectal cancer following chemoradiation therapy: long-term results. *Annals of surgery*. 10 2004;240(4):711–717; discussion 717–718. [PubMed: 15383798]
36. Maas M, Beets-Tan RG, Lambregts DM, et al. Wait-and-see policy for clinical complete responders after chemoradiation for rectal cancer. *Journal of clinical oncology : official journal of the American Society of Clinical Oncology*. 12 10 2011;29(35):4633–4640. [PubMed: 22067400]
37. Martens MH, Maas M, Heijnen LA, et al. Long-term Outcome of an Organ Preservation Program After Neoadjuvant Treatment for Rectal Cancer. *Journal of the National Cancer Institute*. 12 2016;108(12).
38. Sun LL, Yang RY, Li CW et al. Inhibition of ATR downregulates PD-L1 and sensitizes tumor cells to T cell-mediated killing. *American Journal of Cancer Research*. 7 2018;8(7).

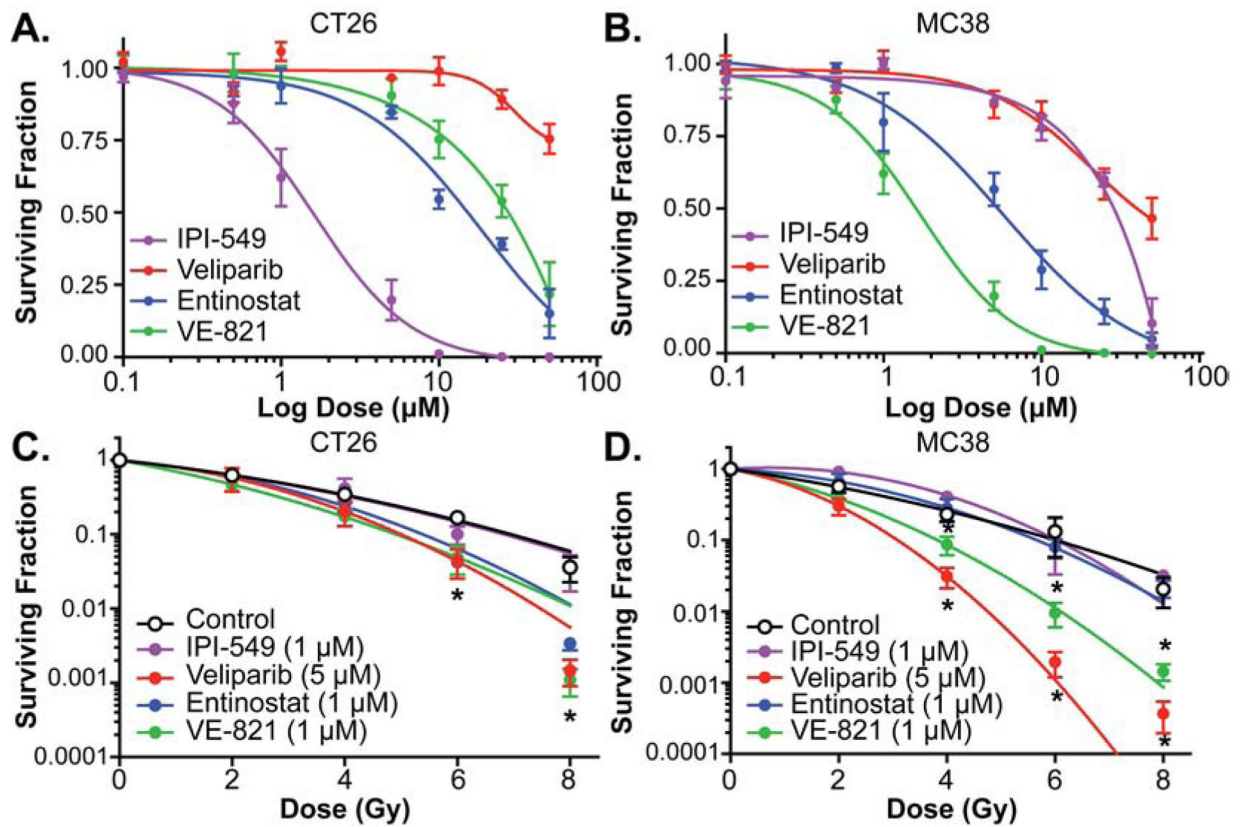


Figure 1: Candidate drug screen.

CT26 (A,C) and MC38 (B,D) cells were treated with varying concentrations of entinostat, IPI-549, VE-821, and veliparib and survival was assessed using clonogenic survival assays to determine IC10 and IC50 values (A-B). Radiosensitization was assessed in both cell lines pretreated with indicated concentrations of each drug and 0–8 Gy of radiation (C-D). Survival was assessed using clonogenic survival assays to determine SER for each drug. N=3–5 for each treatment condition. * indicates $p < 0.05$ compared to control.

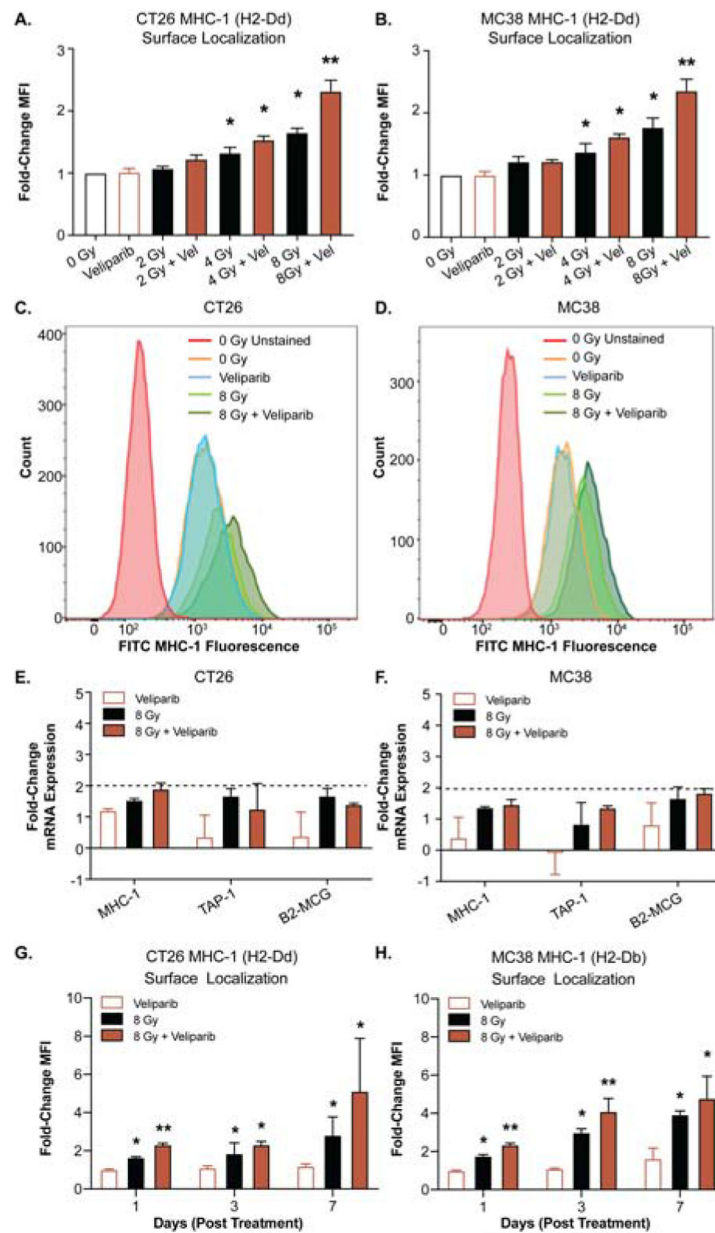


Figure 2: Veliparib pretreatment enhances IR-mediated MHC-1 surface localization.

MHC-1 surface localization was assessed using FLOW cytometry in unpermeabilized cells 24 hours after treatment with a single dose of radiation (0–8 Gy) +/- pretreatment with 5 μ M veliparib. MFIs for MHC-1 H2-D subunit for each condition in CT26 (A) and MC38 (B) cells. Representative histograms are shown for each cell line (C-D). Expression of antigen processing proteins MHC-1 (H2-D subunit), TAP-1, and β 2-macroglobulin was assessed using IR-PCR 24 hours after treatment with 5 μ M veliparib, IR (8 Gy), or both (E-F)). Prolonged surface localization of MHC-1 was assessed by FLOW cytometry in unpermeabilized cells 1, 3, and 7 days after treatment (G-H). N=3–5 for each treatment condition. * indicates $p < 0.05$ compared to control. ** indicates $p < 0.05$ compared to all other groups.

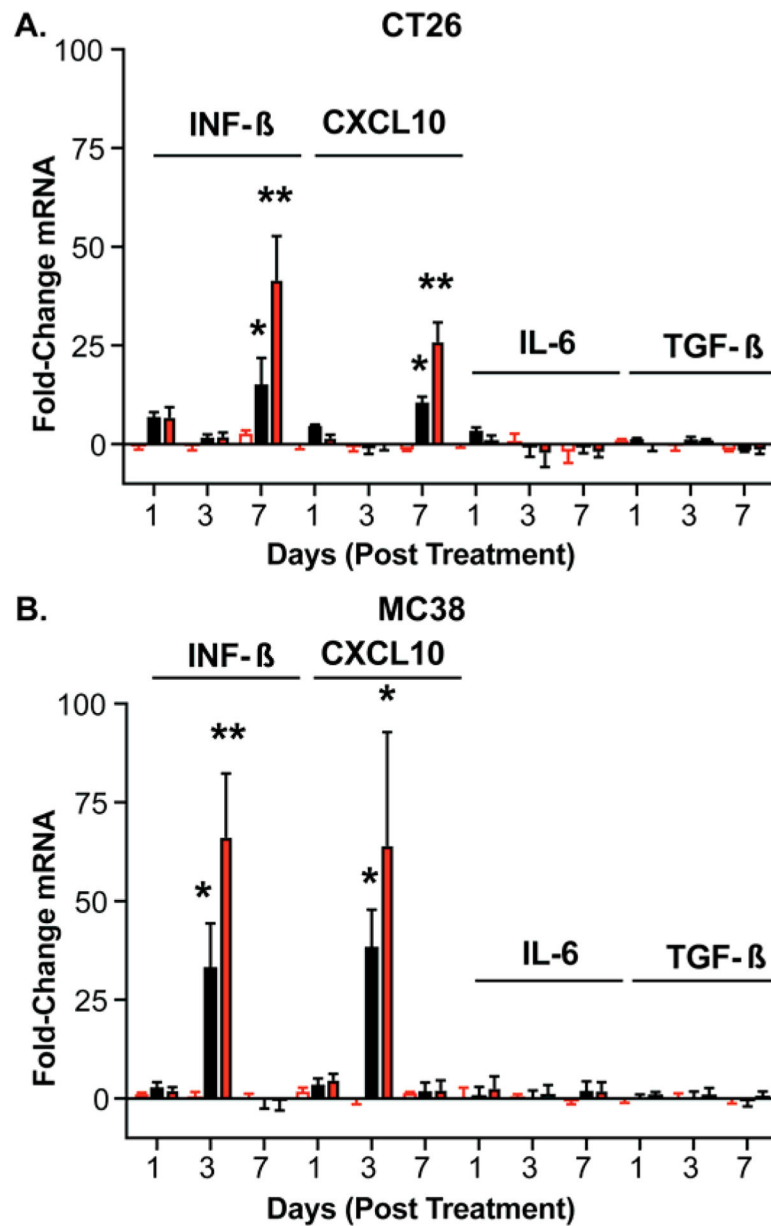


Figure 3: Veliparib enhances delayed expression of inflammatory cytokines and chemokines. Expression of INF-β, CXCL10, IL-6, and TGF-β was assessed 1, 3, and 7 days after treatment with veliparib (5 μM), IR (8 Gy) or both and normalized to untreated controls in CT26 (A) and MC38 (B) cells. N=3 for each treatment condition. * indicates P<0.05 compared to veliparib alone. ** indicates p<0.05 compared to all other groups.

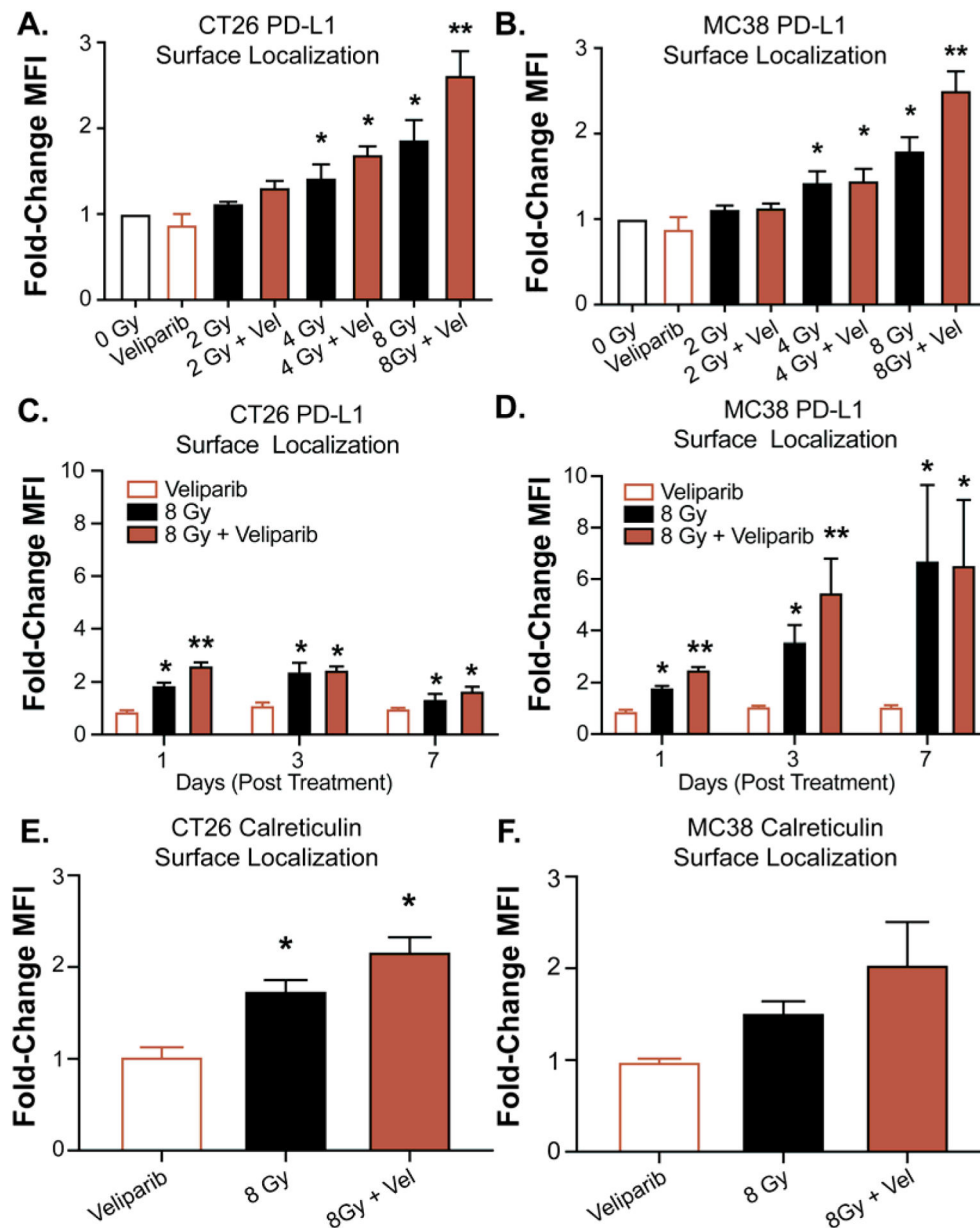


Figure 4: Veliparib enhances IR-mediated surface localization of PD-L1.

PD-L1 surface localization was assessed 24 hours after treatment of radiation (0–8 Gy) +/- veliparib (5 μ M) pretreatment using FLOW cytometry in unpermeabilized cells (A-B).

Prolonged surface localization of PD-L1 was assessed by FLOW cytometry in unpermeabilized cells 72 hours and 1 week after treatment (C-D). Calreticulin surface localization was assessed 24 hours after treatment with drug-free media, veliparib (5 μ M), IR (8 Gy), or both (E-F). N=3–5 for each condition. *Indicates $P < 0.05$ compared to untreated control. **Indicates $p < 0.05$ compared to all other groups.

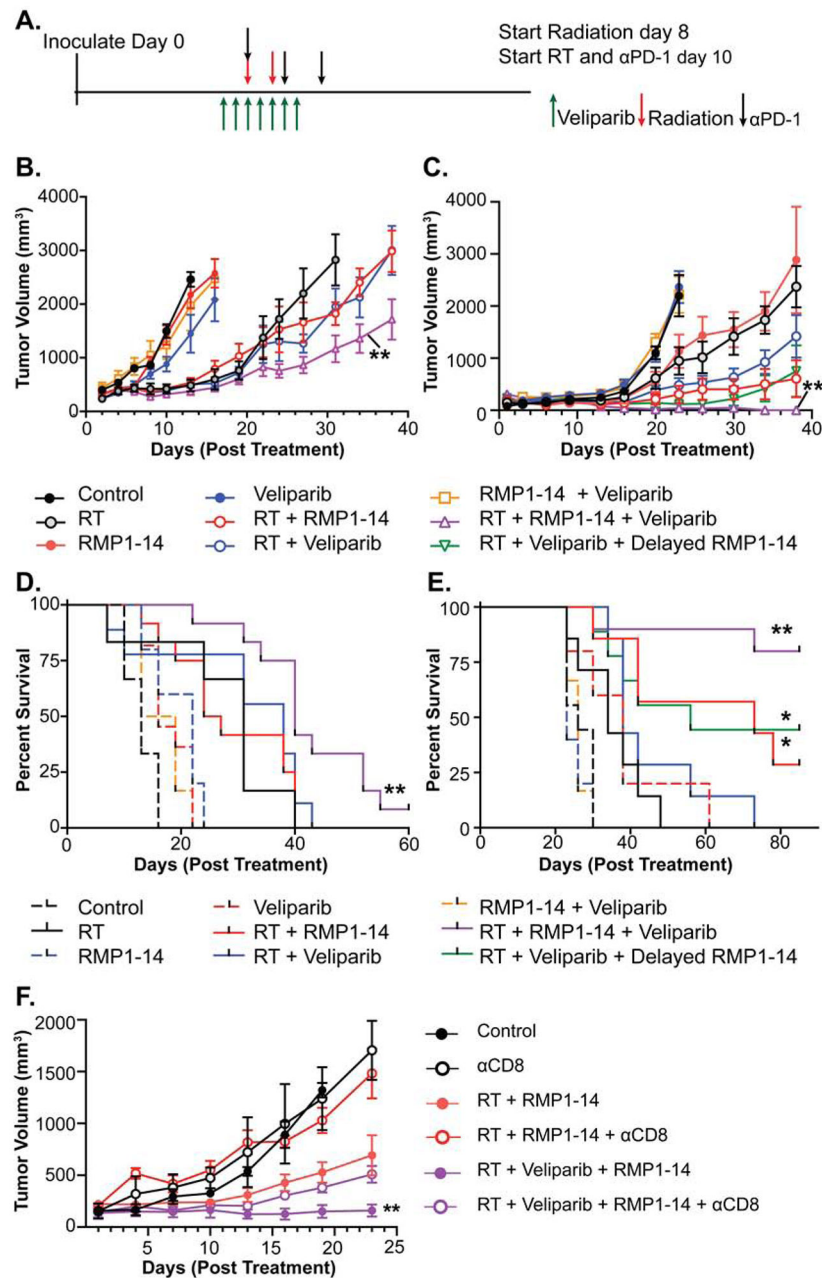


Figure 5: Sub-ablative IR and PARP-inhibition enhance *in vivo* responsiveness to anti-PD-1 antibodies in MSS and MSI tumors.

(A) Schematic representation of the treatment schedule indicating days animals receive veliparib (25 mg/kg BID, green arrows), radiation (8 Gy, red arrows), or RMP1-14 (100 mg/kg IP, black arrows). Tumor volumes following treatment for CT26 and MC38 tumors are shown in (B-C) and survival curves are shown in (D-E). (F) MC38-bearing mice were treated with IR, Veliparib, and RMP-14 +/- CD8+ T-cell depletion. N=3 (control), 5-11 (experimental). *indicates $p < 0.05$ compared to radiation alone. ** indicates $p < 0.05$ compared to all other treatments

Table 1:

Candidate drug monotherapeutic efficacy and radiation sensitization enhancement ratios.

	Drug			
	Veliparib (μM)	Entinostat (μM)	I PI-549 (μM)	VE821 (μM)
CT26				
IC10	11.4	2.1	0.35	3.5
IC50	>100	18.4	1.6	11.9
SER	1.48	1.31	1.05	1.46
MC38				
IC10	5.0	1.1	4.9	0.37
IC50	20.6	6.5	20.7	1.7
SER	1.87	1.05	1.0	1.55

Author Manuscript

Author Manuscript

Author Manuscript

Author Manuscript